Reports

Solar *p*-Mode Eigenfrequencies Are Decreased by Turbulent Convection

Abstract. *Average solar p-mode eigenfrequencies are decreased by large fluctuating velocity fields in the upper convection zone. This effect is greatest for modes with large horizontal wave numbers and frequencies. It is large enough to affect estimates of the depth of the convection zone and may carry useful information about the structure of solar convective turbulence.*

The measured eigenfrequencies of solar *p*-modes have become an important tool for probing the solar interior (*1*). Since the cavity within which these acoustic waves are trapped extends from near the solar surface to a depth that depends strongly on the horizontal wave number k_h (where k_h is inversely proportional to the horizontal wavelength), the variation of the resonant frequencies with k_h can in principle be inverted to yield information on the variation of physical parameters with depth inside the sun. One successful application of such methods seems to be the inference that the solar convection zone extends to a depth of at least 30 percent of the solar radius $R_\odot$, rather than 20 percent or less, as was previously supposed (*2*).

Such inferences are not reliable, however, unless the details of stellar structure and wave propagation within the cavity are correctly treated. Thus uncertainties about the opacity and equation of state can cause uncertainties in the computed frequencies that are large compared to the observational errors (*3*), and variations in the treatment of the upper-boundary condition may have a similar effect (*4*). The variation in the average wave propagation properties inside the sun caused by the turbulent velocity and temperature fluctuations in the upper convection zone constitute a third process for altering the eigenfrequencies; this process has as yet received little attention, even though its effects are comparable to those of the other two (*5*).

The inhomogeneous velocity, density, and temperature distribution in the convection zone modifies the propagation of sound waves in two different ways. The first (which I will not discuss further) is to distort wave fronts passing through the medium, scattering wave energy into different wave numbers than it originally occupied. The second is to change, and in general to slow, the propagation of the mean wave front. To see why this occurs, suppose that the convection produces, in different regions of the fluid, slightly different local wave phase speeds V_{fast} and V_{slow}, symmetrically distributed about some horizontal mean $<V_\phi>$. A wave moves through this medium with a mean speed equal to the distance traveled divided by the total transit time; this mean speed is proportional to

$$\left(\frac{1}{V_{\text{fast}}} + \frac{1}{V_{\text{slow}}}\right)^{-1}$$

The resulting phase speed for the mean wave front is less than $<V_\phi>$ by

$$\frac{(V_{\text{fast}} - V_{\text{slow}})^2}{<V_\phi>}$$

Thus, in a fluctuating medium the mean wave phase speed is not the same as the phase speed in the mean medium.

If we ignore details of reflection at the boundaries, the eigenfrequencies for *p*-modes are those frequencies for which a wave can make a round trip across the cavity in an integral number of wave periods. Other things being equal, lowering the mean wave propagation speed increases this round-trip time and lowers the eigenfrequency.

To quantify these notions and to begin applying them to the sun, consider propagation of infinitesimal disturbances in a medium in which there are small but finite fluctuations in the vertical velocity. (Of course, the solar convection zone also contains fluctuations in the thermodynamic quantities. These are probably unimportant in the current context, but the principal reason for ignoring them is convenience.) To simplify the equations, the solar atmosphere will be taken to be plane-parallel; for the oscillation modes considered, this approximation is quite accurate. Let us denote the unperturbed density by $\bar{\rho}$ and the infinitesimal perturbations in density, pressure, and horizontal and vertical velocity by ρ', p', u' and w', respectively, and allow the finite fluctuating vertical velocity to be W_0. Note that W_0 is defined so that its horizontal average, $<W_0>$, is zero. If spatial and temporal derivatives of W_0 may be ignored, the linearized conservation equations for mass, horizontal and vertical momentum, and energy then read

$$\frac{\partial\rho'}{\partial t} + W_0\frac{\partial\rho'}{\partial z} + w'\frac{d\bar{\rho}}{dz} + \bar{\rho}\left(\frac{\partial w'}{\partial z} + \frac{\partial u'}{\partial x}\right) = 0 \quad (1)$$

$$\bar{\rho}\left(\frac{\partial u'}{\partial t} + W_0\frac{\partial u'}{\partial z}\right) = -\frac{\partial p'}{\partial x}$$

$$g\rho' + \bar{\rho}\left(\frac{\partial w'}{\partial t} + W_0\frac{\partial w'}{\partial z}\right) = -\frac{\partial p'}{\partial z}$$

$$\frac{\partial\rho'}{\partial t} + W_0\frac{\partial\rho'}{\partial z} - \bar{\rho}\frac{N^2}{g}w' = \frac{1}{c^2}\left(\frac{\partial p'}{\partial t} + W_0\frac{\partial p'}{\partial z}\right)$$

Here g is the gravitational acceleration, c is the adiabatic sound speed, and N is the Brunt-Väisälä frequency.

One may factor out the exponential height dependences [see, for example, (*6*)] and Fourier-transform these equations in both spatial dimensions and in time, denoting the temporal frequency by ω and the horizontal and vertical wave numbers by k_h and k_z. Then within a thin slab, in which c^2, N^2, and the density scale height H are sensibly constant, Eqs. 1 may be combined to give a local dispersion relation for acoustic gravity waves. This relation depends on the fluctuating velocity W_0; to obtain the mean dispersion relation one must average over the distribution of W_0 values. Since $<W_0> = 0$ and $|W_0|/c$ is small, it suffices to retain terms of order 0 and 2 in W_0. Then the dispersion relation reads

$$k_z^2 = \left[\!\left[\frac{\omega^2}{c^2} - \frac{\left(1 - \frac{<W_0^2>}{c^2}\right)}{4H^2} - k_h^2\left\{1 - \frac{N^2}{\omega^2}\left[1 + \frac{<W_0^2>}{\omega^2}\left(5\,k_z^2 - \frac{1}{4H^2}\right)\right]\right\}\right]\!\right] \times \left(1 - \frac{<W_0^2>}{c^2}\right)^{-1} \quad (2)$$

If $<W_0^2> = 0$, Eq. 2 reduces to the well-known dispersion relation for acoustic-gravity waves. Such waves may propagate vertically only if k_z^2 is positive; otherwise the waves are evanescent. Within the solar envelope and for reasonable values of k_h and ω, $k_z^2 > 0$ within a bounded region (or cavity) below the photosphere. The positions of the upper and lower edges of this cavity depend on k_h, ω, and the solar structure, and are termed the upper and lower turning points for the waves in question.

Including fluctuating vertical velocities evidently changes the dispersion relation in three ways: it increases k_z^2, it lowers the effective acoustic cutoff frequency, and it modifies the effect of buoyancy forces on the wave propagation. The first two of these effects are consistent with lowering the local wave propagation speed by a factor $1 - (\langle W_0^2 \rangle / c^2)$.

When the differential equation corresponding to Eq. 2 is supplemented by appropriate boundary conditions (vanishing pressure perturbation at the surface and vanishing velocity perturbation at depth), its solutions provide the eigenfunctions and eigenfrequencies for solar p-modes within an envelope with fluctuating vertical velocities. One may estimate the importance of the velocity fluctuations by comparing solutions with and without the vertical velocities, giving eigenfrequencies denoted by ω_p and ω_0, respectively.

The model envelope used to calculate eigenfrequencies is crude but adequate for the purpose of comparing solutions with and without velocity fluctuations. The mean stratification is assumed to be plane-parallel, with the gravitational acceleration, the adiabatic exponent Γ_1, and the molecular weight all constant with depth. The envelope is adiabatically stratified below a reference level $z = 0$ and isothermal above that level, with the model parameters chosen to give a fair approximation to accurate models of the solar envelope. The p-mode frequencies computed by use of the model agree with those observed on the sun to within about 10 percent. Below $z = 0$, turbulent velocities for computing the perturbed eigenfrequencies come from a solar model provided by R. Gilliland. This model uses a standard mixing-length formulation to compute root-mean-square (r.m.s.) velocities. The resulting r.m.s. velocity distribution reaches a rather sharp peak of about 2 km $\sec^{-1}$ near $z = -600$ km. Above $z = 0$, the r.m.s. velocity is set to a constant 1 km $\sec^{-1}$, corresponding to photospheric granulation velocities.

This model illustrates most of the important physics, but I emphasize that accurate computations must treat the geometry, ionization, and radiative transfer correctly. Fortunately, neither a precise model of the sun nor accurate agreement with observed oscillation frequencies is necessary for the current purpose. Preliminary results of calculations done in collaboration with B. W. Mihalas show qualitatively similar effects.

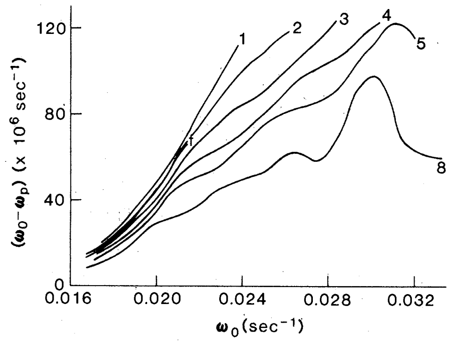

Fig. 1. Difference between eigenfrequencies ω_0 and ω_p computed, respectively, without and with vertical turbulent velocities, plotted as a function of ω_0. The frequencies with turbulent motions are always smaller than those without, leading to positive differences.

The differences between frequencies computed without and with vertical velocities are shown in Fig. 1 for the f mode and for p modes 1 through 5 and 8. Including the effect of vertical velocities lowers the p-mode frequencies by amounts as large as 1.2×10^{-4} $\sec^{-1}$, or about 0.5 percent of the unperturbed frequency. The greatest differences occur for modes with large ω or k_h. This happens because $\langle W_0^2 \rangle$ is large only in a shallow layer near the top of the envelope, with the maximum amplitude falling above the upper turning point for most of the modes plotted here. For a given wave number, increasing ω raises this turning point, so that more of the large-amplitude portion of the eigenfunction lies within the region of large convective velocities. If ω is large enough, the upper turning point can be raised so far that the eigenfunction's first node falls at the maximum of $\langle W_0^2 \rangle$. In this case (illustrated by the $n = 8$ curve above $\omega = 0.03$), the influence of the turbulent velocities is sharply reduced. Increasing k_h raises the lower turning point of the oscillations, causing the eigenfunctions to become more concentrated near the surface. This also accentuates the effect of the turbulent velocities.

Though not large by absolute standards, 0.5 percent variations in p-mode frequencies are significant when compared with observational errors and have noticeable implications concerning the structure of the solar interior. As discussed by Ulrich and Rhodes (*2*), the frequencies at large k_h are a sensitive indicator of the entropy in the convection zone. Within the mixing-length formalism, increasing α (the ratio of the mixing length to the pressure scale height) leads to a deeper convection zone with larger convective velocities. Increasing the depth of the convection zone in turn lowers the computed p-mode eigenfrequencies. In order to get frequencies similar to those observed, Lubow *et al.* (*3*) found that their model indicates that α must be about 1.65, corresponding to a convection zone depth of about 0.27 $R_\odot$.

However, including convective fluctuations in the calculation of p-mode eigenfrequencies lowers those frequencies still further. To bring the computed frequencies back into agreement with observation, one must decrease α. Estimates based on the analysis by Ulrich and Rhodes suggest that raising the frequencies by 0.5 percent requires decreasing α to 1.45. This corresponds to a convection zone depth of about 0.24 $R_\odot$. Though the absolute value of the convection zone depth (and especially the absolute value of the mixing length) estimated in this way are open to doubt, the magnitude and sense of the changes implied by considering vertical velocities in the analysis are probably correct. A more thorough treatment, including horizontal velocities and temperature variations, might easily double the size of this effect.

Within the frequency range covered by observations, the frequency shifts caused by vertical flows have a form similar to those produced by variations in α. This will make disentangling the two effects less clear-cut and will thus increase the difficulty in arriving at an unambiguous picture of the sun's internal structure. However, careful observations (particularly at high ω) may allow one to separate the turbulent contribution. One might therefore learn something about the variation of convective velocities just below the photosphere independent of estimates of the total depth of the convection zone, providing a means for testing theories of convection.

TIMOTHY M. BROWN

High Altitude Observatory, National Center for Atmospheric Research, Post Office Box 3000, Boulder, Colorado 80307

References and Notes

1. D. Gough, *Phys. Bull.* **34**, 502 (1983).
2. R. Ulrich and E. Rhodes, *Astrophys. J.* **218**, 521 (1977).
3. S. Lubow, E. Rhodes, R. Ulrich, in *Nonradial and Nonlinear Stellar Pulsations*, H. Hill and W. Dziembowski, Eds. (Springer, New York, 1980), p. 300; A. Noels, R. Scuflaire, M. Gabriel, *Astron. Astrophys.* **130**, 389 (1984).
4. R. Rosenwald and H. Hill, in *Nonradial and*

Nonlinear Stellar Pulsations, H. Hill and W. Dziembowski, Eds. (Springer, New York, 1980), p. 404.
5. However, for treatments that are similar in spirit, see J. Logan, H. Hill, P. Puccio, and R. Rosenwald [in *Nonradial and Nonlinear Stellar Pulsations*, H. Hill and W. Dziembowski, Eds. (Springer, New York, 1980), p. 413] and B. Durney [in *Proceedings of the Snowmass Conference on Observing Solar Oscillations from Space*, R. Ulrich, Ed. (in press)].
6. B. Mihalas and J. Toomre, *Astrophys. J.* **249**, 349 (1981).
7. I thank R. Gilliland for allowing me to use his solar mixing-length results and B. Mihalas for many useful discussions.

6 June 1984; accepted 25 July 1984

Periodicity of Extinctions in the Geologic Past: Deterministic Versus Stochastic Explanations

Abstract. *The temporal spacing and the magnitude of major extinctions over the past 250 and 570 million years, based on the use of different metrics of extinction probability, are analyzed by comparing deterministic and stochastic explanations. The best-fitting time series model is a stochastic autoregressive model that displays a pseudoperiodic behavior with a cycle length of 31 million years for the past 250 million years, regardless of the metric of extinction probability. The periodicity lengthens and weakens when the analysis is extended to the entire Phanerozoic. The history of the probability of extinction for the entire Phanerozoic, based on time series analysis, does not support the reported bipartite distribution of Van Valen. Rather, the probability of extinction has decreased uniformly over Phanerozoic time whereas the inertia or stability of the biotic system after the Late Permian crisis has increased.*

The probability of extinction is known to have been nonconstant over geologic time (*1*). Fischer and Arthur (*2*) proposed that major extinction events (*3*) have occurred periodically. Raup and Sepkoski (*4*) recently applied statistical tests for periodicity to a data set of 567 extinct marine families whose origination and extinction times can be resolved to a geologic stage (mean duration, 6.2 million years). These analyses, restricted to the window of geologic time from 253 to 11.3 million years ago, identified 12 extinction peaks whose temporal spacing was significantly periodic at 26 million years. Raup and Sepkoski interpreted these results as a signal of an unknown event that appears uniformly and suggested astrophysical causes.

The periodicity described by Raup and Sepkoski compels attention. Our objectives are threefold: (i) to broaden the statistical analysis and thereby the interpretation of these data by comparing deterministic versus stochastic explanations, including models with and without external forcing functions; (ii) to focus on a neglected aspect of the data—namely, the striking feature that the magnitude of extinction peaks varies from 7.6 to 66.3 percent; and (iii) to broaden the empirical support by applying these alternative models to Van Valen's metrics (*5*), which differ substantially in the method of calculating the probability of extinction.

An observed periodicity in a given time series, evidenced as a peak in the spectrum or autocorrelation function of the series, could be the result of three very different causes (*6*): (i) a deterministic impulse which affects the evolution of the series only at specific times with fixed periodicity; (ii) a deterministic cycle in which some external variable follows a periodic wave which affects the evolution of the series; or (iii) a stochastic dynamic system (the stochastic behavior may be the result of multiple unknown causal factors operating to produce the observed series). In the first two cases, the periodic behavior observed can only be explained as a result of the effect of some exogenous variable. In the third case, to restrict our search to an external cause may be misleading, whereas attention to the internal structure of the system might increase our understanding of the observed behavior.

To test these alternatives statistically, we have first applied a series of models to the data of Raup and Sepkoski. The results are summarized in Table 1. Model 1A represents the series modeled as a response to a deterministic impulse function. The parameter value that takes into account this deterministic effect is not significant. To allow for the observed autocorrelation in the series, model 1B adds a stochastic term. Although the capacity of explanation of the model increases, this is not due to the deterministic component which is still not significant. We also checked the presence of deterministic sinusoidal components fitting autoregressive-integrated-moving-average (ARIMA) models (*6*) that allow for cancellation of the roots in the autoregressive polynomials (*7*), but we have not detected any indication of this kind of behavior. Model 2 is the best stochastic representation of the series, based on the use of ARIMA time-series models, that we have obtained and displays periodic (pseudoperiodic) behavior (*8*). This model is a fifth-order autoregressive model, that is, a model in which the current value of the series is explained as a linear combination of its values in the five previous periods. In this case, the parameter values obtained from maximum likelihood estimation are such that they produce pseudocyclic behavior. To test robustness to the apparent outlying observation (the Late Cretaceous extinction event), we also fitted the models using intervention analysis (*9*). These conclusions were also robust, and model 3 represents the best-fitted model. Although such an intervention model has a greatly increased capacity of explanation ($R^2 = 0.71$), taking into account this effective outlier does not change the basic pseudoperiodic behavior referred to above. Figure 1 illustrates the observed series, including the variable magnitudes

Table 1. Models for the Late Permian–Middle Miocene time series of extinction probability, using the Raup-Sepkoski metric (*4*). Abbreviations: B is the backshift operator $B^k Y_t = Y_{t-k}$, and $\nabla = 1 - B$ is the difference operator; Y_t is the observed series; X_t is some deterministic series of zeros and ones with the ones separated by five stages; a_t is a white-noise process of uncorrelated variables with zero mean and constant variance. The parenthetical numbers under the estimated parameters are the t-statistics for these parameters. Q is the Ljung-Box statistic (11 degrees of freedom); δ is the residual estimated variance of the model; R^2 is the percentage of explained sum of squares; and I is an intervention variable that takes the value 1.0 in period 30 (Late Cretaceous) and 0 elsewhere.

Estimated model	$Q(11)$	δ_a^2	R^2
1A. $Y_t = 16.88 + 4.5\,X_t + a_t$ (6.82) (0.82)	19.6	190.0 (169.5)	0.02
1B. $Y_t = 16.7 - 1.29\,X_t + (1 - 0.32B)^{-1} a_t$ (5.62) (0.29) (2.33)	10.0	145.0	0.25
2. $(1 + 0.66B + 0.56B^2 + 0.71B^3 + 0.38B^4)\nabla Y_t = a_t$ (4.2) (3.8) (4.6) (2.56)	6.2	122.8	0.45
3. $Y_t = 42.68 I_{30} + \dfrac{a_t}{\nabla(1 + 0.32B + 0.56B^2 + 0.45B^3 + 0.22B^4)}$ (6.71) (1.94) (3.75) (2.71) (1.55)	4.1	63.65	0.71